Universitat de Girona

Mohammad Hosein Naserian

Hot-press postprocessing of 3D-printed composites for improved interlaminar fracture toughness and healing

FRP++
Advanced structural analysis and design using composite materials

Master Dissertation
European Master Advanced Structural Analysis and Design using Composite Materials

Work developed under the supervision of
Dr. Norbert Blanco Villaverde
Dr. Dani Trias Mansilla

Funded by the European Union

September 2025

DECLARATION

Name: Mohammad Hosein Naserian

Email: mhnaserian@yahoo.com

Title of the Dissertation: Hot-press postprocessing of 3D-printed composites for improved interlaminar fracture toughness and healing

Supervisors:

Dr. Norbert Blanco Villaverde

Dr. Dani Trias Mansilla

Year of Conclusion: 2025

Master Course in Advanced Structural Analysis and Design using Composite Materials

University of Girona, 01/09/2025

Signature:

ACKNOWLEDGEMENTS

This research was funded by the Spanish Ministry of Science, Innovation and Universities (MCIU), the Spanish Research Agency (AEI) and the European Regional Development Fund (FEDER, UE) (grant no. PID2022-140343NB-100)

I want to thank FRP++ Program and both University of Minho and University of Girona for providing this unique opportunity. It was all I expected and more.

I want to thank my supervisors, Prof. Norbert Blanco and Dani Trias, for trusting me working on an interesting state-of-the-art project, and assisting me by all means during this journey.

I want to thanks Dr. Alex Fernandez and Dr. Daniela Rico for guiding me through the work and sharing their individual experiences with me. It made the journey a lot easier.

I want to thank Mr. Marti Descamps, AMADE's lab technician, who was providing means for conducting the tests and analysis.

Next, I want to extend this thanks to my friends who helped me with all they could.

Finally, I want to thank my family. If Mohammad Hosein is graduated today, it is because of their sacrifices and unconditional supports. I hope one day I can make it up for you.

Posprocesamiento mediante prensado en caliente de compuestos impresos en 3D para mejorar la tenacidad y la reparación de grietas interlaminares

RESUMEN

Este trabajo tiene como objetivo estudiar las propiedades de tenacidad a la fractura interlaminar de materiales compuestos CCF/PA6 producidos mediante fabricación aditiva, y también investigar la posibilidad de reparar una grieta interlaminar mediante el uso de las capacidades de reparación de la matriz termoplástica. Las muestras se dividieron aleatoriamente en dos grupos. El primer lote no fue posprocesado excepto por el corte a las dimensiones finales de ensayo. El segundo lote fue posprocesado a 130°C, y 0.5 MPa durante 30 minutos, lo que en promedio disminuyó el espesor del segundo lote en un 16.7%. Los dos grupos se ensayaron siguiendo la norma ASTM D5628 para la caracterización en modo I de la tenacidad interlaminar. Después del ensayo, el lote posprocesado mostró un aumento del 10% en $G_{\mathrm{IC-Iniciación}}$ seguido de una disminución del 5% en $G_{\mathrm{IC-Propagación}}$ en comparación con el primer lote, que no fue posprocesado. Después de realizar la etapa de reparación de la grieta a 180°C y 0.250 MPa durante 60 minutos, se observó que es posible reparar una grieta interlaminar. Esto se pudo comprobar llevando a cabo análisis de termografía por infra-rojos antes y después de cada etapa de posproceso y ensayo. El valor de $G_{\mathrm{IC-Iniciación}}$ tras la reparación fue prácticamente el mismo en el segundo lote, pero con una disminución del 23.6 % en el primero. Sin embargo, ambos grupos experimentaron una disminución significativa en su $G_{\mathrm{IC-Propagación}}$. Esta disminución fue del 86 % en el primer lote y del 75 % en el segundo, en comparación con su estado inicial. En comparación entre sí, las muestras posprocesadas presentaron valores de $G_{\mathrm{IC-Iniciación}}$ un 40 % más altos y un 69 % más altos para $G_{\mathrm{IC-Propagación}}$. Las mediciones dimensionales de las probetas mostraron que tras la reparación se produjo un incremento en todas las dimensiones del primer lote: 1.6 % en grosor, 2.3 % en anchura y 0.8 % en longitud. En el segundo lote se observó una disminución del 2.5 % en grosor fue seguida por un aumento del 12.3 % en anchura, sin cambios significativos en la longitud de las muestras.

PALABRAS CLAVE: Tenacidad a la fractura interlaminar modo I; posprocesamiento; fibra de carbono continua; fabricación aditiva; reparación.

Postprocessament mitjançant premsat en calent de materials compostos impresos en 3D per millorar la tenacitat i la reparació de fractures interlaminars

RESUM

Aquest treball pretén estudiar les propietats de tenacitat a la fractura interlaminar de materials compostos CCF/PA6 produïts mitjançant fabricació additiva, i també investiga la possibilitat de reparar una esquerda interlaminar mitjançant les propietats de reparabilitat de la matriu termoplàstica. Les mostres es van dividir aleatòriament en dos grups. El primer lot no va ser postprocessat excepte pel tall segons les dimensions finals d'assaig. El segon lot es va postprocessar a 130°C i 0.5 MPa durant 30 minuts, cosa que en promig va reduir el gruix d'aquest segon grup en un 16.7%. Els dos grups es van assajar seguint la norma ASTM D5628 per a la caracterització en mode I de la tenacitat interlaminar. Després dels assaigs, el lot postprocessat va mostrar un augment del 10% en $G_{\mathrm{IC-Iniciació}}$ seguit d'una disminució del 5% en $G_{\mathrm{IC-Propagació}}$ en comparació amb el primer lot que no es va postprocessar. Després de realitzar la fase de curació a 180°C i 0.250 MPa durant 60 minuts, es va observar que és possible la reparació d'una esquerda interlaminar. Això es va comprovar mitjançant anàlisis de termografia per infra-rojos de les provetes abans i després de cada etapa de post-processat i assaig. El valor de $G_{\mathrm{IC-Iniciació}}$ després de la fase de reparació va ser aproximadament el mateix per al segon lot, però amb una disminució del 23.6% per al primer lot. No obstant això, ambdós grups van experimentar una disminució important en la seva $G_{\mathrm{IC-Propagació}}$. Aquesta disminució va ser del 86% per al primer lot i del 75% per al segon lot, en comparació amb el seu estat inicial. I en comparació entre si, les mostres postprocessades van presentar valors un 40% més alts de $G_{\mathrm{IC-Iniciació}}$ i un 69% més alts de valors de $G_{\mathrm{IC-Propagació}}$. Les mesures de dimensionals de les provetes van mostrar que després de la reparació es va produir un increment en totes les dimensions del primer lot: un 1.6% en gruix, un 2.3% en amplada i un 0.8% en longitud. En el segon lot es va observar una disminució del 2.5% en gruix, seguida d'un augment del 12.3% en amplada i cap canvi important en la longitud de les mostres.

PARAULES CLAU: Mode de tenacitat a la fractura interlaminar I; postprocessament; fibra de carboni contínua; fabricació additiva; reparación.

Hot-press postprocessing of 3D-printed composites for improved interlaminar fracture toughness and healing

ABSTRACT

This work aims to study the interlaminar fracture toughness properties of additive manufactured CCF/PA6 composites, and also, investigates the possibility of healing a progressed interlaminar crack by using the repairability properties of thermoplastic matrix. The specimens were randomly divided into two groups. The first batch was not post-processed in any way except for cutting them to the final test dimensions. The second batch was post-processed at 130°C and 0.5 MPa for 30 min, which on average implied a 16.7% decreased the thickness of the first batch. The two groups were then tested following the ASTM D5528 standard for the characterization of the mode I interlaminar fracture toughness. After testing, the post-processed batch showed a 10% increase in $G_{\mathrm{IC-Initiation}}$ followed by a decrease of 5% in $G_{\mathrm{IC-Propagation}}$ in comparison to the first batch, which was not post-processed. After performing the healing stage at 180°C and 0.25 MPa for 60 min, it was observed that healing an interlaminar crack is possible. This was confirmed by conducting an infra-red thermal analysis before and after every post-processing step and test. The $G_{\mathrm{IC-Initiation}}$ value after the healing stage was roughly the same for the second batch, but with 23.6% drop for the first batch. However, both groups experienced a major decrease in their $G_{\mathrm{IC-Propagation}}$. A drop of 86% for the first batch and 75% for the second batch when compared to their primary state. In comparison with each other, post-processed specimens presented 40% higher values of $G_{\mathrm{IC-Initiation}}$ and 69% of higher values of $G_{\mathrm{IC-Propagation}}$. The dimension measurements showed that after healing all dimensions increased for the first batch: 1.6% in thickness, 2.3% in width and 0.8% in length. For the second batch, a decrease of 2.5% in thickness was followed by an increase of 12.3% in width, and no major change in length of the specimens

KEYWORDS: Interlaminar fracture toughness mode I; post-processing; continuous carbon fiber; additive manufacturing; healing.

TABLE OF CONTENTS

LIST OF FIGURES

LIST OF TABLES

List of Abbreviations and Symbols

Abbreviations

CCF	Continuous Carbon Fiber
PA6	Polyamide 6
DCB	Double Cantilever Beam
HP	Hot Press
MBT	Modified Beam Theory
FDM	Fused Deposition Modelling
CAD	computer-aided design

Symbols

$G_{\mathrm{IC-Initiation}}$	Fracture toughness initiation (Critical energy release rate)
$G_{\mathrm{IC-Propagation}}$	Fracture toughness propagation (Critical energy release rate)

THIS PAGE WAS INTENTIONALLY LEFT BLANK

1. INTRODUCTION

1.1. Motivation

Continuous Carbon Fiber (CCF) has been a good solution for manufacturers whenever a higher value of performance to weight was required. However, producing parts with conventional methods have some major setbacks like being prone to human-error and a time-consuming manufacturing process. Newer methods like Automated Fiber Placement solved these problems, but there are expensive and unfeasible for a limited number of productions. During the past two decades, it has been a growing interest in additive manufacturing (AM) due to its unique features: the ability of rapid prototyping, being a cheap option compared to the advanced methods, and the ability to print complex geometries are a few to mention [1], [2], [3]. Nevertheless, the problem associated with additive manufacturing of composite materials is the higher value of void contents when compared to the conventional methods: around 10% for AM compared to a maximum of about 5% [4]. These voids affect the mechanical performance of the structure, so researchers have tried to improve the part's performance by various means, from changing the nozzle head shape to changing the printing bed temperature.

Previous studies have used a hot-press process to improve interlaminar fracture toughness. In this study, the main objective is to use a hot-press to weld and heal interlaminar cracks present in the laminate after testing. To the best knowledge of the author, this is a novel and unexplored approach. Therefore, the literature review will be focused on applying Hot-Press (HP) as post-processing.

1.2. Objectives

One of the unique aspects of using thermoplastic matrices is their ability to get remelted and repaired [5], [6]. Prior researchers have tried compression moulding to acquire superior mechanical properties. However, the main objective in this study is to take advantage of the thermoplastic matrix and investigate the possibility of healing a progressed interlaminar crack by using a hot-press and put it into testing again to compare the after-healing interlaminar fracture toughness with the initial results.

The side objectives will be optimization of the variables for compression moulding process such as temperature, pressure, and duration of the process.

1.3. Structure of the Dissertation

After delving into previously published literature, experimental procedures in this study will be elaborated, followed by the results and discussions. At the end, conclusion and suggestions for future works will be presented.

2. LITERATURE REVIEW

In this section, additive manufacturing (AM) for composites and the previous studies on post-processing of 3D-printed parts will be presented. The major focus will be toward the studies using hot-press as their post-processing. Their results will be mentioned here and discussed in the next chapters.

2.1. Additive Manufacturing

Additive manufacturing, also known as 3D-Printing, is a technology for manufacturing products layer by layer from a computer-aided design (CAD) model. Its popularity is due to its fast and cheap way of manufacturing [7], [8]. As demand for customized parts is growing, researchers try to improve the AM methods and remove the constraints along the way to manufacture products with higher qualities in terms of surface finish, structural strength, etc [9], [10]. Fused deposition modelling (FDM), or addressed as fused filament fabrication (FFF), is the most used AM technology due to the previously mentioned reasons and the ease of use [2]. Nonetheless, there has been a concern about the stiffness and strength of products produced by FDM [11].

2.2. Effect of microscopic voids on mechanical performance

After printing 24 layers of continuous carbon fiber and putting an insert in the middle, DCB arrangement, He et al. [1] exposed some of the specimens to a pressure of 5 MPa for 10 minutes at 230°C. The results indicated that the volume fraction of voids decreased from 12.5% to 5.9%. Additionally, the value for fracture toughness initiation ($G_{\mathrm{IC-Initiation}}$) increased from 118 to 225 J/m^2. However, the value for $\mathrm{G_{IC-Propagation}}$ had a major decrease from 1467 to 472 J/m^2. This effect was attributed to the lack of fiber bridging phenomena. Fiber bridging is a toughening mechanism in fiber-reinforced composite where fibers across a delamination crack, resisting the opening of the crack and slowing the propagation [12]. Additionally, voids and irregularities not only were acting as barriers by preventing the matrix to transfer the stress, but also, making the fiber bridging more likely to happen. Hou et al. [13] also reported higher fracture toughness at propagation for DCB specimens with the higher volume of voids, as the interlaminar voids in different planes were contributing to the two above mentioned factors and dissipating more energy [14].

2.3. Post-processing and dimensional behaviour

Previous studies had reported an oversized dimensional error about 4 times higher for the z axis than the one for the xy plane in desktop 3D-Printers [15], [16]. However, Pascual-González et al. [17] found a dimensional error of 10% for the z-axis, which was higher than the almost -0.5% reported for their xy plane. A hypothetical idea justifying this error is about the difficulty of printing continuous carbon fiber. In overall, the results are compatible with other studies that evaluated dimensional accuracy of 3D-Printed parts. Pascual-González et al. tried post processing the specimens in a wide range of temperatures from 70°C to 270°C, with applying a pressure equal to 1 MPa for 15 minutes. As the temperature increased, the thickness also decreased. It is worth mentioning that the attempt to post process the specimens at 270°C failed as the temperature and pressure caused overflowing the coupon during the treatment and loss its original shape. As the study mentions, post processing compensates for the deviation in z direction, and the values obtained after post processing in 130°C and 150°C are closer to the nominal value than the untreated sample, Figure 2.1.

The C-scan of treated specimens at 130°C showed that the attenuation increases from the center to the edges, indicating the movement of trapped air towards the edges from the center. Further images showed that the central area of coupons treated at 150°C and 170°C were properly consolidated, although there was still considerable amount of entrapped air close to the edges.

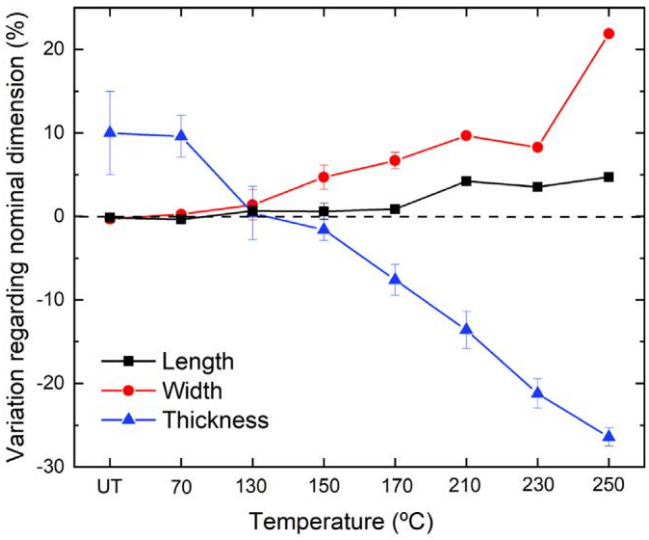

Figure 2.1 Dimension variation for specimens post-processed at different temperatures [17]

By using X-ray computed tomography it was shown the treatment at 70°C did not affect the porosity volume in specimens but it makes them to distribute evenly in the specimen. The photos also confirmed that the voids are located between traces and layers but not within the filaments, as previous studies reported [18].

2.4. Other literatures and methods

In 2022, Saeed et al. [19] tried to increase the fiber fraction volume in specimens by using two methods: 1- varying the number of fiber layers in the specimens. 2- using a hot-press at 130°C to improve the fiber-matrix bonding and decreasing the voids. After applying 50 bars of pressure and holding the specimens under the pressure for 1 hour, specimens were tested. The result showed an increase of 27% in tensile strength and elastic modulus compared to those of unpressed specimens. Furthermore, micro-sectioning images showed the void content of unidirectional specimens reduced from 3.96% to 0.26%, which is equivalent of producing the specimens by using the conventional methods, Figure 2.2.

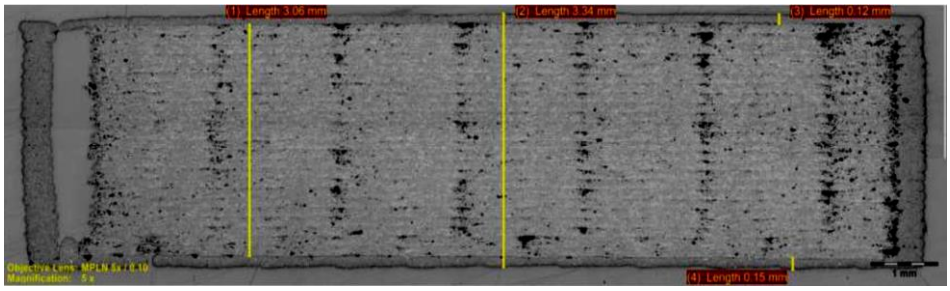

(a)

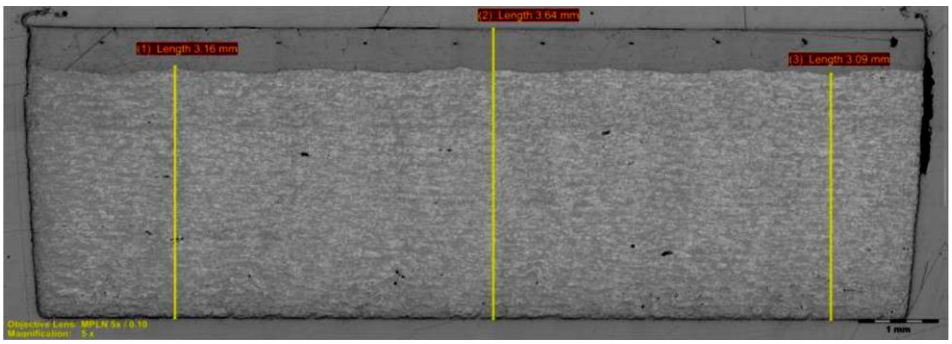

(b)

Figure 2.2 Void content analysis for (a) non-pressed (b) pressed specimens [19]

Although the flexural behaviour of a material is highly affected by its intralaminar and interlaminar fracture toughness, there are not many literatures available on this matter [20].Aliheidari et al. [21] were one of the first researchers to characterize additive manufactured specimens of neat ABS to improve the fracture toughness in mode I. They found that the higher the extrusion temperature, the higher the fracture resistance, with maximum reported values close to the fracture resistance of bulk ABS. In another work, Farmand-Ashtiani et al. [22] studied the effect of thickness DCB in composite specimens. They recorded no effect of thickness on the initiation value of fracture toughness while the propagation value tended to increase with the thickness. Researchers have tried to improve the mechanical properties by different means. Goh et al. [23] found the highest fracture toughness of G_{IC} = 943 J/m^2 for the CCF specimen manufactured at low printing speed of 7 mm/s, with heated bed at 70°C and nozzle temperature of 265°C [24]. Zhu et al. [25] proposed an ultrasound and plasma assisted additive manufacturing method. The effect of each physical field was investigated solely, and it came out by increasing the power of both, the voids content is tended to decrease more. Then, in a synergic study, both fields were applied at the same time. The results indicated both factors are acting in the same way. The final results showed a reduction of more than 6 times for the treated specimens compared to untreated ones, and the interlaminar shear performance was improved more than 50%.

3. MATERIALS AND METHODS

Polyamide (PA), or Nylon, offers better stiffness and strength compared to polyethylene (PE) or polypropylene (PP). When it is reinforced by fibers, it becomes a good candidate for load bearing applications and structural components. Whereas its melting point is around 215-220°C, it performs well in high temperatures up to 200°C [26].

3.1. 3D printer, Materials, and manufacturing constraints

The specimens in this study were manufactured by using a desktop Mark Two® 3D-printer from Markforged company. This 3D printer has been widely used in similar studies due to the rare feature of printing continuous carbon fiber. The printer has two nozzle heads: one for printing Nylon (Polyamide 6 or addressed as PA6) or a combination of PA6 with short carbon fiber (named as Onyx) and one for printing the fiber. This apparatus opposes some constraints to its users: (i) fixed printing parameters, such as temperature, printing speed and layer thickness; (ii) restricted printable materials (only Markforged proprietary materials); (iii) the inability to only print reinforced material. Indeed, PA6 contours, roof and floor layers are added in all specimens by default [17].

The CCF/PA6 specimens printed in this study had the following characterization: (i) Unidirectional CCF in longitudinal direction; (ii) 100% infill rate to achieve solely testing the reinforced material; (iii) The Nylon floor and roof were removed after printing and later specimens were cut to remove any possible remaining.

3.2. Specimen design

The design comprised of 24 layers of unidirectional carbon fiber for Double Cantilever Beam (DCB) structure. The direction of the rasters was longitudinal and parallel to the intended crack propagation direction. First, to ensure the proper adhesion of fibers to the bed, the Markforged imposed to print at least two layers of Nylon before printing the reinforced material. Hence, initially two layers of Nylon were printed ($220\ \mathrm{mm} \times 51\ \mathrm{mm}$). Subsequently, 12 layers of unidirectional continuous carbon fiber ($180\ \mathrm{mm} \times 31\ \mathrm{mm}$) were printed in longitudinal direction, followed by the application of a thin Kapton® film to serve as a precrack for DCB testing, Figure 3.1. Afterward, another 12 layers were

printed to ensure a symmetrical layup Figure 3.1. Each layer of CCF and Nylon has the same thickness of 0.125 mm. Later, after printing, the PA floor was removed. The procedure applied in this study and the specimen design was similar to other studies [20].

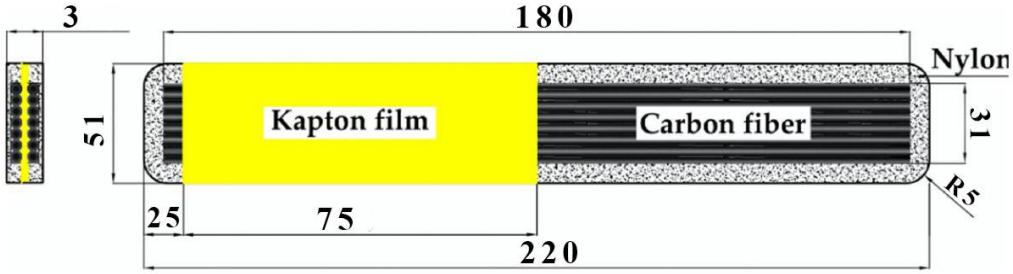

Figure 3.1 Specimen schematic and dimensions [20]

3.3. Specimen preparation and testing

Afterwards, in order to prepare the specimens for testing the printed specimens were cut with a diamond saw to the final dimensions of $173\ \mathrm{mm} \times 25\ \mathrm{mm}$. Then, the top and bottom surfaces of the specimens were polished using fine sand papers to ensure better adhesion of loading blocks. Blocks were attached to the specimens by a strong epoxy adhesive, LOCTITE® EA 9497. The tests were performed under ASTM D5528 [27] standard to obtain the mode I interlaminar fracture toughness values. The loading and unloading speeds were 5 and 25 mm/min, respectively. Tests were executed at room temperature.

3.4. Post-processing

After printing 14 specimens, two groups of seven specimens were randomly selected. Later, the first batch was tested without any initial post-processing, while the second batch was post-processed. The reason behind separating specimens in two groups is to compare the performance of initially post-processed specimens to those holding their original form after printing. The same comparison will be extended among the two groups by investigating the fracture toughness properties for the after-healing stage.

Post-processing may lead to higher mechanical properties related to the reduction in void content, but it introduces a new step in the manufacturing process which increases the time and cost of manufacturing specimens. Also, using a hot-press process causes shape modification, which requires further actions to obtain the desired final geometry.

The post-process characterization consists of pressure, temperature, duration of which the specimens will be kept under the press, and the velocity of heating up and cooling down were defined by considering the knowledge shared by previous studies present in the literature (Section 2).

Although using higher pressures can lead to higher mechanical properties, excessive pressure has two major setbacks: (i) pressure accompanied by temperature can remove most of the void content but it also prevents the positive fiber bridging phenomena to happen [1]; (ii) it can disrupt the continuous carbon fiber path and cause premature failure [19]. Therefore, a pressure of 0.5 MPa at 130°C and 30 minutes of holding time was considered for the post-processing of the second batch of the specimens. The heating and cooling rates were set to 10°C/min and 20°C/min, respectively. The values were consistent with those mentioned by other articles and the constraints of the hot-press machine available for this study.

Finally, readers should know that the first batch is addressing the non-processed specimens and the second batch is addressing the processed specimens.

3.5. Healing process

As previously mentioned, remelting and repairing of thermoplastic matrices by applying heat cycles that can be repeated is one of the unique aspects of using a thermoplastic matrix. By using this feature, all the specimens in this research were exposed to a healing stage. The Table 3.1 shows the different possibilities for the healing process. These options were considered by taking into account the characterization used in other reports.

Table 3.1 Possibilities for hot-press healing characterization

Temperature (°C)	Pressure (MPa)	Duration (min)	Velocity of heating (°C/min)	Velocity of cooling (°C/min)
180	0.25	60	10	20
180	1	60	10	20
223	1	30	10	20
200	2	30	10	20
200	5	10	10	20

Before confirming the final characterization for doing the healing process for all the specimens, the process was performed on random samples one by one. The first specimen failed due to applying more pressure than the limit. The second specimen was healed at 180°C and 1MPa for one hour. The thermography analysis confirmed the success of healing process. However, the thickness had been reduced about 30% after performing healing, which was more than the acceptable range of this study. As a result, the third specimen was healed at the lowest pressure possible according to the system used, and after verification by thermal analysis, the same settings were considered for healing of the rest of specimens. Hence, all the samples experienced heating at 180°C for one hour and a pressure of 0.25 MPa.

The reason behind the selection of the lowest temperature and pressure possible was due to the less chance of failure for the specimens as other reports mentioned high temperature and pressure caused material overflow and failure of the specimen. In addition, higher pressures decrease thickness of the laminate too much which is unfavorable for fracture toughness.

It must be mentioned that due to some operational issues, the first batch of specimens was heated one time up to 180°C and cooled down naturally to prevent any residual stresses in specimens. During this incident neither any pressure was applied to the specimens, nor they were exposed to the heat for a long time because the process was monitored constantly and it was stopped immediately after the malfunction was recognized.

Worth of mention is that, before and after performing each step, thermal images were taken using a FLIR T560 camera to observe the changes. These images were later processed by ImageJ software and will be presented in the next chapter.

3.6. Experimental setup

The tests to determine the mode I fracture toughness were conducted following the ASTM D5528 [15] standard. Loading and unloading was performed by an MTS Insight 5kN at 5 and 25 mm/min, respectively. During precrack and propagation phases, the interlaminar crack was monitored and pictures of the crack tip were regularly captured every half a second using a Canon 550D + macro EF100 setup to help recording the details and identifying crack propagations. A Zeiss Stemi DV4 / DR was used for better identifying the measurement of the crack length before and after the tests. Last but not least, a Fontijnepresses LabEcon 300 kN hot-press machine used for post-processing and healing of the specimens. The maximum heating up and cooling down velocities for this machine were 10°C/min and 20°C/min respectively.

4. RESULTS AND DISCUSSIONS

4.1. Healing a progressed crack

In order to qualitatively assess the extension of the interlaminar crack surface and the healing effect, an infra-red thermographic analysis was carried out. The analysis was based on heating the specimens with heat pulses generated by two halogen lamps in one surface of the specimen and monitoring with the infra-red camera the temperature evolution in the other surface of the specimen. Because the thermal conductivity of the material of the specimen is higher than the thermal conductivity of air, in those areas without interlaminar crack the temperature increase was faster than in those areas where delamination was present.

Before starting the process, thermographic images of the specimens were taken. Later, after post-processing, testing and healing new thermographic images were taken. One specimen from each batch is selected to show the changes during these processes. Figure 5.1 shows the thermographic images of those specimens. Since for the first batch, the thermal images were not taken before the first test, specimen 756 was selected as the representative of all the specimens after printing. Then, the left branch is presenting the thermal variation of the non-processed specimens (first batch) and the right branch is presenting the thermographic images of the processed specimens (second batch). The remaining images are presented in the appendix I. In the most cases, both groups presented similar homogenized thermal conductivities. The delamination is visible after testing in both specimens. The photos in the post-processed batch appeared brighter indicating a better internal connection among the components and, consequently, a better heal. Shortly after, this idea confirmed by the second batch showing around 50% higher fracture toughness properties than the first batch.

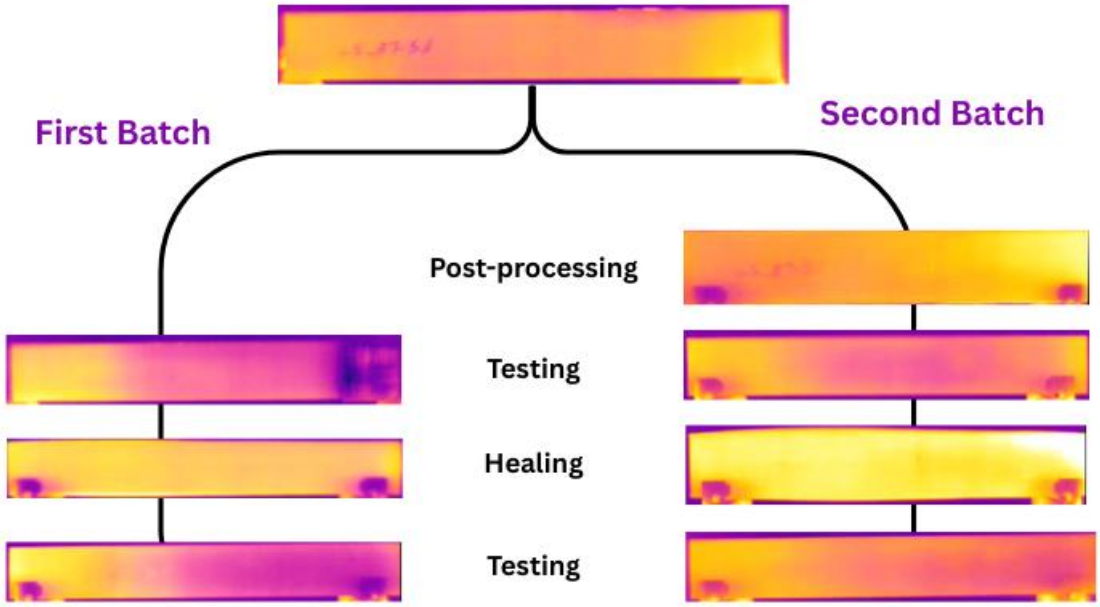

Figure 4.1 Thermal analysis of specimens during the study. Left) Specimen 747 and Right)756

4.2. Fracture toughness analysis

Following the ASTM D5528 standard [27], a precrack between 3 and 5 mm was generated from the insert, following the same testing procedure to avoid any effect of not having a sharp crack tip or resin pocket at the end of the insert. Figure 4.2 shows the load-displacement curves during propagation phases. At first, the first batch showed higher loads during propagation phases, but less displacements than the second batch. Moreover, the postprocessed batch data showed less dispersion. After healing, the post-processed batch presented both higher loads and displacements than the first batch. The values for both groups were considerably higher during the primary tests. The stick-slip behaviour was observed more in the post-processed batch. After healing stage, this phenomenon increased in number and happened repetitively.

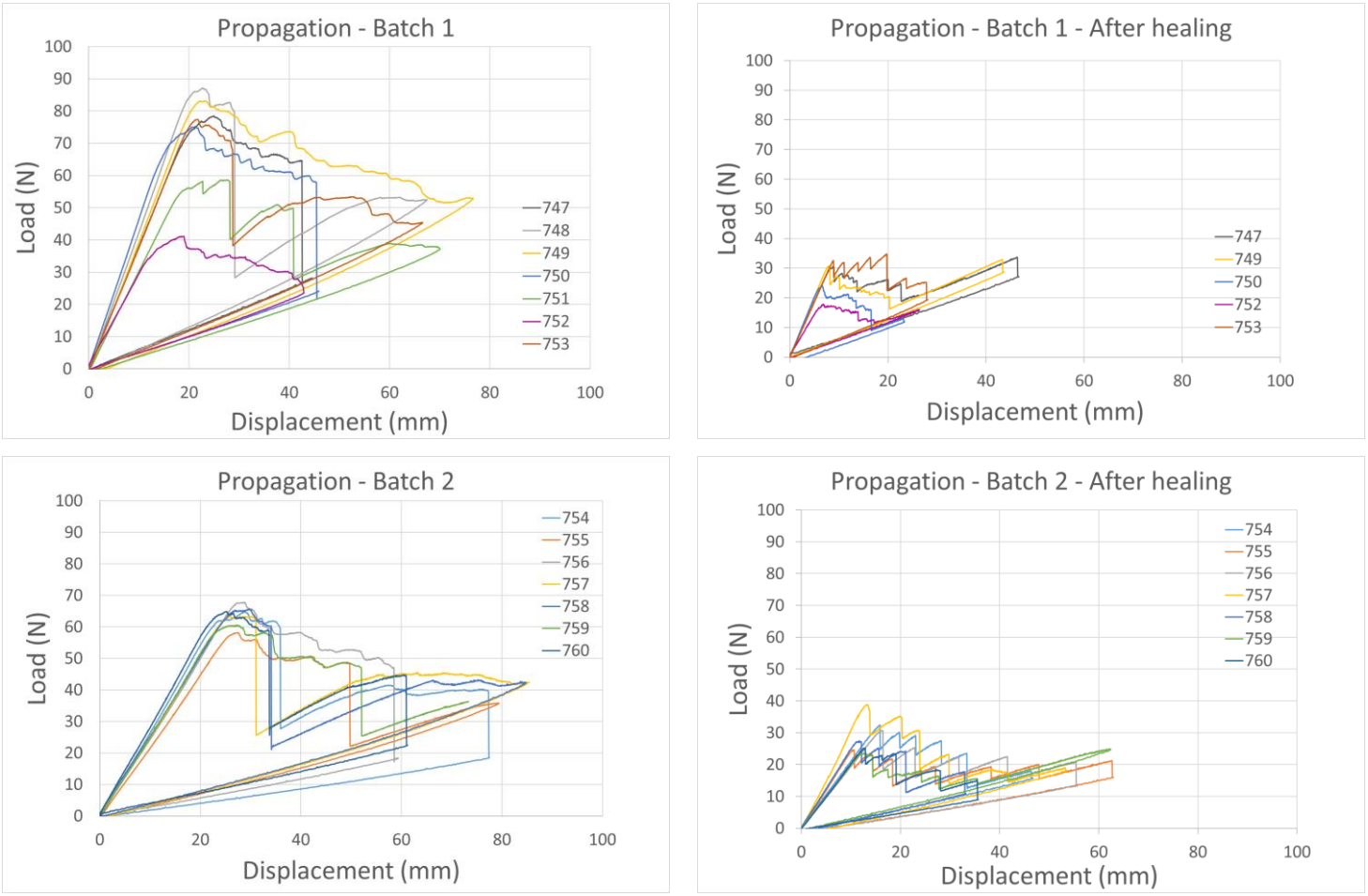

Figure 4.2 Propagation charts before and after healing. Top) Batch 1 (non-postprocessed specimens) and Bottom) Batch 2 (postprocessed specimens)

The primary values for the fracture toughness of the two groups were calculated based on Modified Compliance Calibration (MCC) method as indicated in the standard, and are presented in the Table 4.1.

Table 4.1 Interlaminar fracture toughness initiation and propagation values of specimens before and after healing

	Before healing		After healing	
Name	$G_{\mathrm{IC-initiation}}$ (J/m²)	$G_{\mathrm{IC-propagation}}$ (J/m²)	$G_{\mathrm{IC-initiation}}$ (J/m²)	$G_{\mathrm{IC-propagation}}$ (J/m²)
First batch	161 ± 9.85	1666 ± 241	123 ± 35.4	230.9 ± 80.7
Second batch	176 ± 10	1597 ± 196	173 ± 77.9	389 ± 120.9

It can be observed in the table that the specimens after compression moulding presented higher initiation values with lower propagation values, as other studies in the literature already reported [1]. However, the difference between the values reported here was not as severe as the differences reported by He et al. [1]: an increase of 90% for initiation values with a drop of 70% in propagation values for the post-processed

specimens. In this work, an increase of 10% in initiation value was accompanied by a decrease of 5% in propagation value. After healing, both groups presented lower values of interlaminar fracture toughness than their primary states in the most cases. The propagation value dropped by 86% for the first batch and 76% for the second batch. For the initiation value, the first batch experienced a drop of 23.6% while the initiation value for the post-processed specimens was the only factor that remained the same, with on average only 1.7% decrease after healing.

4.3. Dimensional changes

4.3.1. Thickness variation

After post-processing, the thickness of the specimens decreased by 17% on average, followed by an increase in the other two dimensions. Table 4.2 shows the dimensional changes after post processing the specimens. A similar tendency was observed after performing the healing phase. The thickness decreased 2.5% on average.

Table 4.2 Thickness change for the post-processed specimens (batch 2) after post-processing and healing

Specimen	Starting (mm)	After PP (mm)	Change	After healing (mm)	Change
754	3.09	2.63	-14.89%	2.69	+2.28%
755	3.07	2.61	-14.98%	2.61	0.00%
756	3.24	2.59	-20.06%	2.52	-2.70%
757	3.3	2.62	-20.61%	2.48	-5.34%
758	3.3	2.63	-20.30%	2.58	-1.90%
759	3.07	2.65	-13.68%	2.61	-1.51%
760	3.09	2.71	-12.30%	2.48	-8.49%

After healing stage, the measurements showed a slight increase, on average 1.6%, in the thickness of the non-postprocessed specimens (first group), Table 4.3. A similar behaviour was reported by Pascual-Gonzalez et al. [17], considering that post-processing helped an even distribution of trapped air within the specimens rather than removing it.

Table 4.3 Thickness change for the first batch after healing

Specimen	Starting (mm)	After healing (mm)	Change
747	3.28	3.34	-1.83%
748	3.37	Failed[1]	-
749	3.38	3.46	-2.37%
750	3.31	3.35	-1.21%
751	3.27	Failed	-
752	3.06	3.24	-5.88%
753	3.33	3.22	3.30%

Figure 4.4 shows the evolution of thickness in both groups.

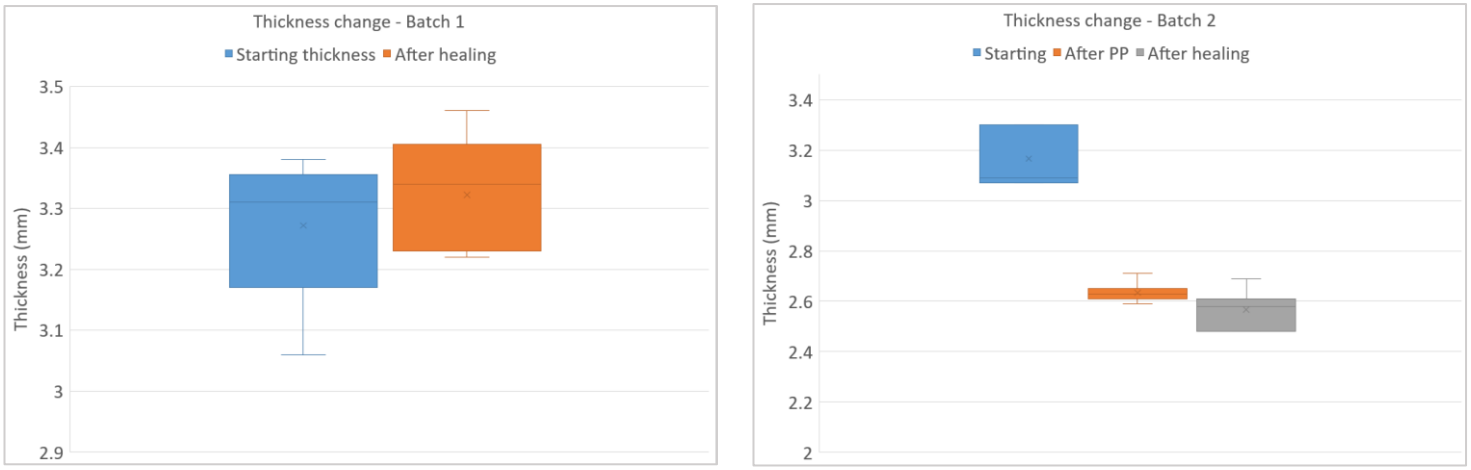

Figure 4.3 Thickness variation before and after hot-press process. Left) Batch 1 and Right) Batch 2

[1] In fact, the specimen 748 was not failed. It was just healed under a different pressure. However, in order to prevent readers from distraction, it was addressed as a failed specimen. The final after healing thickness for this specimen was 2.36 mm.

4.3.2. Width and length variation

After healing, the width and length of non-processed batch increased by 2.3% and 0.8%, respectively. Table 4.4 shows the variation of width and length for each specimen.

Table 4.4 Width and length variation after healing for non-postprocessed batch

	Width			Length		
Specimen	Starting (mm)	After healing (mm)	Change	Starting (mm)	After healing (mm)	Change
747	24.45	24.72	+1.10%	171.43	172.83	+0.82%
748[2]	24.45	Failed	-	171.9	Failed	-
749	24.36	24.62	+1.07%	171.75	172.96	+0.70%
750	24.58	24.45	-0.53%	172.19	173.56	+0.80%
751	24.27	Failed	-	172.62	Failed	-
752	24.52	25.39	+3.55%	173.15	174.69	+0.89%
753	24.4	25.64	+5.08%	172.9	174.3	+0.81%
Mean			+2.05			+0.8

Next, Table 4.5 is presenting the width and length variation for the post-processed specimens before and after each process. The average width variation after post-processing was 14.9% and after healing 12.3%. Both values were considerably larger than the variations recorded for the length, 0.3% after PP and 0.1% after healing. Comparing the width variation with the other group, width variation in the post-processed specimens after healing is more than five times more that of the non-postprocessed. One the other hand, the increase in length of post-processed specimens is ten times less than non-postprocessed batch.

Table 4.5 Width and length variation for the post-processed specimens after each process

	Width						Length				
Specimen	Starting (mm)	After P.P (mm)	Change	Cutting (mm)	After healing (mm)	Change	Starting (mm)	After P.P (mm)	Change	After healing (mm)	Change
754	25.24	28.63	+13.43%	25.11	29.2	+16.29%	173.19	173.47	+0.16%	173.66	+0.11%
755	25.2	29.1	+15.48%	25.09	28.6	+13.99%	172.97	173.41	+0.25%	173.6	+0.11%
756	25.07	29.54	+17.83%	25.25	29.48	+16.75%	172.91	173.51	+0.35%	173.5	+0.01%
757	25.08	29.39	+17.19%	25.23	28.03	+11.10%	172.5	172.83	+0.19%	173.03	+0.12%
758	25.22	29.57	+17.25%	24.98	27.55	+10.29%	172.8	173.48	+0.39%	173.41	+0.04%
759	25.27	28.6	+13.18%	24.98	25.81	+3.32%	172.91	173.39	+0.28%	173.37	+0.01%
760	25.34	27.81	+9.75%	25.05	28.57	+14.05%	172.87	173.3	+0.25%	173.44	+0.08%
Mean			+14.9			+12.3			+0.3		+0.1

[2] The specimen 748 did not failed, but it was processed in different pressure, so its value is not presented in the table. After healing width was equal to 31.05 mm and after healing length was 173.31 mm.

Lastly, Figure 4.4 shows the specimen 760 as a representative of all the specimens after healing. It is clearly visible that the specimen underwent an inhomogeneous width change. Each arm has their own width and the maximum width is somewhere in between. Therefore, all the specimens were cut in order to maintain the same geometry and be ready for the fracture toughness tests.

Figure 4.4 Inhomogeneous width variation after healing

5. CONCLUSIONS AND FUTURE WORKS

5.1. Conclusions

In this study, CCF/PA6 laminates were fabricated using FDM technology to be utilized for further characterization of interlaminar fracture toughness mode I. DCB specimens with a symmetrical composite lay-up were divided into two groups. The first batch stayed in its original form after printing whereas the second group experienced an optimized hot-press post-processing at 130°C, 0.5 MPa for 30 minutes. This post-processing later led to superior performance of the second batch in most cases. A 10% increase in fracture toughness initiation value for post-processed specimens was accompanied by less than five percent decrease in its propagation value, compared to the specimens tested at their primary state. The second achievement of this study was the balanced results between initiation and propagation value of the post-processed specimens. While similar work of He et al. [1] reported a 90% increase in the initiation value of their compression moulded specimens, it was coupled by almost a 70% loss of the propagation value. This behaviour was not observed in this study suggesting the possibility of further optimization of the post-processing settings without extreme loss of mechanical properties.

The state-of-the-art idea of healing a progressed crack using the unique properties of thermoplastic matrices in repairing was tested and confirmed. Nonetheless, further work in this area is demanded, the post-processed batch offered an initiation value as high as the first result. The propagation value dropped by 75% and 86%, respectively for the second batch and first batch.

5.2. Future works

As the study confirms the possibility of healing a progressed crack, further research on optimization of the healing process and the post-process are needed. Further research can study the healing possibility and performance of the specimens for mixed mode fracture toughness.

REFERENCES

[1] Q. He, H. Wang, K. Fu, and L. Ye, "3D printed continuous CF/PA6 composites: Effect of microscopic voids on mechanical performance," *Compos Sci Technol*, vol. 191, 2020, doi: 10.1016/j.compscitech.2020.108077.

[2] B. N. Turner, R. Strong, and S. A. Gold, "A review of melt extrusion additive manufacturing processes: I. Process design and modeling," 2014. doi: 10.1108/RPJ-01-2013-0012.

[3] C. K. Chua, K. F. Leong, and C. S. Lim, *Rapid prototyping: Principles and applications, third edition*. 2010. doi: 10.1142/6665.

[4] R. Protz, N. Kosmann, M. Gude, W. Hufenbach, K. Schulte, and B. Fiedler, "Voids and their effect on the strain rate dependent material properties and fatigue behaviour of non-crimp fabric composites materials," *Compos B Eng*, vol. 83, 2015, doi: 10.1016/j.compositesb.2015.08.018.

[5] J. D. Muzzy and A. O. Kays, "Thermoplastic vs. thermosetting structural composites," *Polym Compos*, vol. 5, no. 3, 1984, doi: 10.1002/pc.750050302.

[6] G. Jogur, A. Nawaz Khan, A. Das, P. Mahajan, and R. Alagirusamy, "Impact properties of thermoplastic composites," *Textile Progress*, vol. 50, no. 3, 2018, doi: 10.1080/00405167.2018.1563369.

[7] Y. Huang *et al.*, "Force-Based Adaptive Deposition in Multi-Axis Additive Manufacturing: Low Porosity for Enhanced Strength," 2025. doi: 10.2139/ssrn.5146382.

[8] X. Zhang, W. Fan, and T. Liu, "Fused deposition modeling 3D printing of polyamide-based composites and its applications," 2020. doi: 10.1016/j.coco.2020.100413.

[9] D. Ahlers, F. Wasserfall, N. Hendrich, and J. Zhang, "3D printing of nonplanar layers for smooth surface generation," in *IEEE International Conference on Automation Science and Engineering*, 2019. doi: 10.1109/COASE.2019.8843116.

[10] G. Fang, T. Zhang, S. Zhong, X. Chen, Z. Zhong, and C. C. L. Wang, "Reinforced FDM: Multi-axis filament alignment with controlled anisotropic strength," *ACM Trans Graph*, vol. 39, no. 6, 2020, doi: 10.1145/3414685.3417834.

[11] W. Zhong, F. Li, Z. Zhang, L. Song, and Z. Li, "Short fiber reinforced composites for fused deposition modeling," *Materials Science and Engineering: A*, vol. 301, no. 2, 2001, doi: 10.1016/S0921-5093(00)01810-4.

[12] R. Khan, "Fiber bridging in composite laminates: A literature review," 2019. doi: 10.1016/j.compstruct.2019.111418.

[13] M. Hou, L. Ye, and Y. W. Mai, "Effect of moulding temperature on flexure, impact strength and interlaminar fracture toughness of CF/PEI composite," *Journal of Reinforced Plastics and Composites*, vol. 15, no. 11, 1996, doi: 10.1177/073168449601501104.

[14] M. Mehdikhani, L. Gorbatikh, I. Verpoest, and S. V. Lomov, "Voids in fiber-reinforced polymer composites: A review on their formation, characteristics, and effects on mechanical performance," 2019. doi: 10.1177/0021998318772152.

[15] M. N. Islam, B. Boswell, and A. Pramanik, "An investigation of dimensional accuracy of parts produced by three-dimensional printing," in *Lecture Notes in Engineering and Computer Science*, 2013.

[16] G. W. Melenka, J. S. Schofield, M. R. Dawson, and J. P. Carey, "Evaluation of dimensional accuracy and material properties of the MakerBot 3D desktop printer," *Rapid Prototyp J*, vol. 21, no. 5, 2015, doi: 10.1108/RPJ-09-2013-0093.

[17] C. Pascual-González *et al.*, "Post-processing effects on microstructure, interlaminar and thermal properties of 3D printed continuous carbon fibre composites," *Compos B Eng*, vol. 210, 2021, doi: 10.1016/j.compositesb.2021.108652.

[18] C. Pascual-González, M. Iragi, A. Fernández, J. P. Fernández-Blázquez, L. Aretxabaleta, and C. S. Lopes, "An approach to analyse the factors behind the micromechanical response of 3D-printed composites," *Compos B Eng*, vol. 186, 2020, doi: 10.1016/j.compositesb.2020.107820.

[19] K. Saeed *et al.*, "Characterization of continuous carbon fibre reinforced 3D printed polymer composites with varying fibre volume fractions," *Compos Struct*, vol. 282, 2022, doi: 10.1016/j.compstruct.2021.115033.

[20] J. D. Santos, A. Fernández, L. Ripoll, and N. Blanco, "Experimental Characterization and Analysis of the In-Plane Elastic Properties and Interlaminar Fracture Toughness of a 3D-Printed Continuous Carbon Fiber-Reinforced Composite," *Polymers (Basel)*, vol. 14, no. 3, 2022, doi: 10.3390/polym14030506.

[21] N. Aliheidari, R. Tripuraneni, A. Ameli, and S. Nadimpalli, "Fracture resistance measurement of fused deposition modeling 3D printed polymers," *Polym Test*, vol. 60, 2017, doi: 10.1016/j.polymertesting.2017.03.016.

[22] E. Farmand-Ashtiani, J. Cugnoni, and J. Botsis, "Specimen thickness dependence of large scale fiber bridging in mode I interlaminar fracture of carbon epoxy composite," *Int J Solids Struct*, vol. 55, 2015, doi: 10.1016/j.ijsolstr.2014.03.031.

[23] G. D. Goh, V. Dikshit, J. An, and W. Y. Yeong, "Process-structure-property of additively manufactured continuous carbon fiber reinforced thermoplastic: an investigation of mode I interlaminar fracture toughness," *Mechanics of Advanced Materials and Structures*, vol. 29, no. 10, 2022, doi: 10.1080/15376494.2020.1821266.

[24] J. D. Santos, S. Fotouhi, J. M. Guerrero, and N. Blanco, "Characterization of the mixed-mode interlaminar fracture toughness of an additive manufacturing continuous carbon fiber reinforced-thermoplastic composite," *Polym Compos*, vol. n/a, no. n/a, Apr. 2025, doi: https://doi.org/10.1002/pc.29943.

[25] W. Zhu *et al.*, "Synergistic interlaminar strengthening of high-content continuous fiber reinforced composites via ultrasound and plasma-assisted 3D printing," *Compos Sci Technol*, vol. 263, p. 111079, 2025, doi: https://doi.org/10.1016/j.compscitech.2025.111079.

[26] U. K. Vaidya and K. K. Chawla, "Processing of fibre reinforced thermoplastic composites," 2008. doi: 10.1179/174328008X325223.

[27] American Society for Testing and Materials, *ASTM D5528-13. Standard Test Method for Mode I Interlaminar Fracture Toughness of Unidirectional Fiber-Reinforced Polymer Matrix Composites*. 2022.

APPENDIX I

Thermal photos

The first batch: specimen 0747 to 0753 and the second batch is from 0754 to 0760.

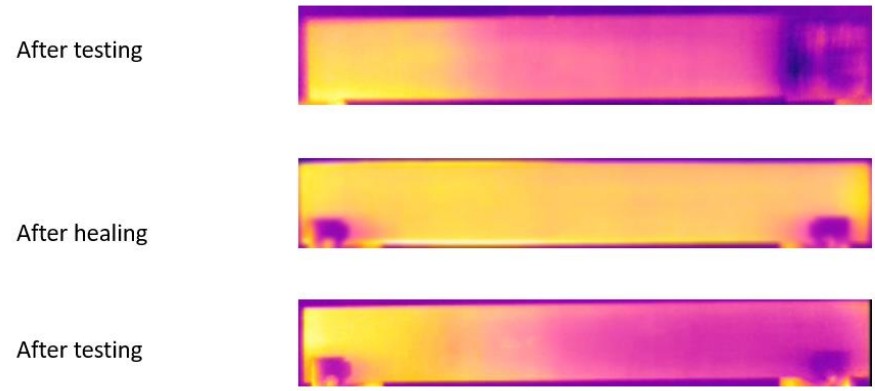

Figure 5.1 Specimen 0747 thermal photos

Figure 5.2 Specimen 0748 thermal photos

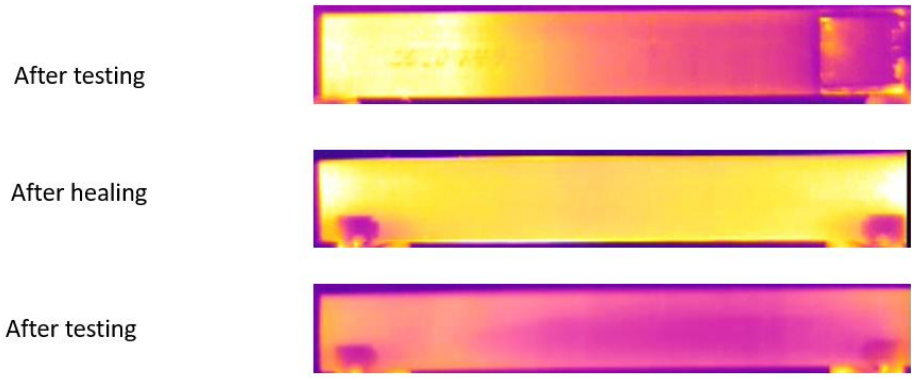

Figure 5.3 Specimen 0749 thermal photos

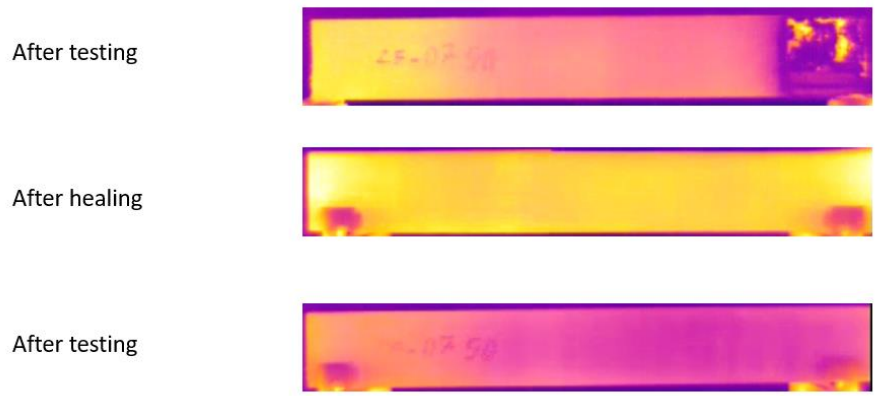

Figure 5.4 Specimen 0750 thermal photos

Figure 5.5 Specimen 0751 thermal photos

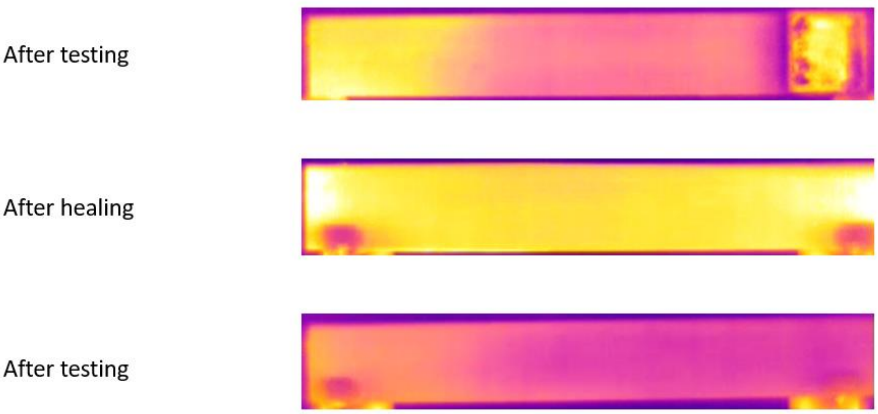

Figure 5.6 Specimen 0752 thermal photos

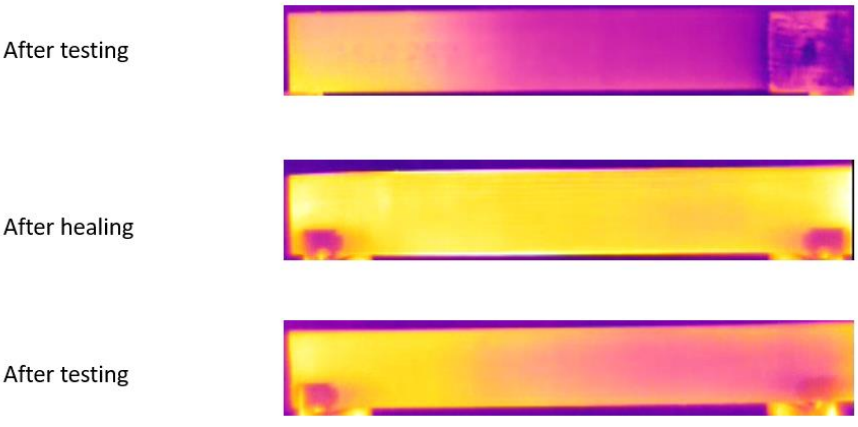

Figure 5.7 Specimen 0753 thermal photos

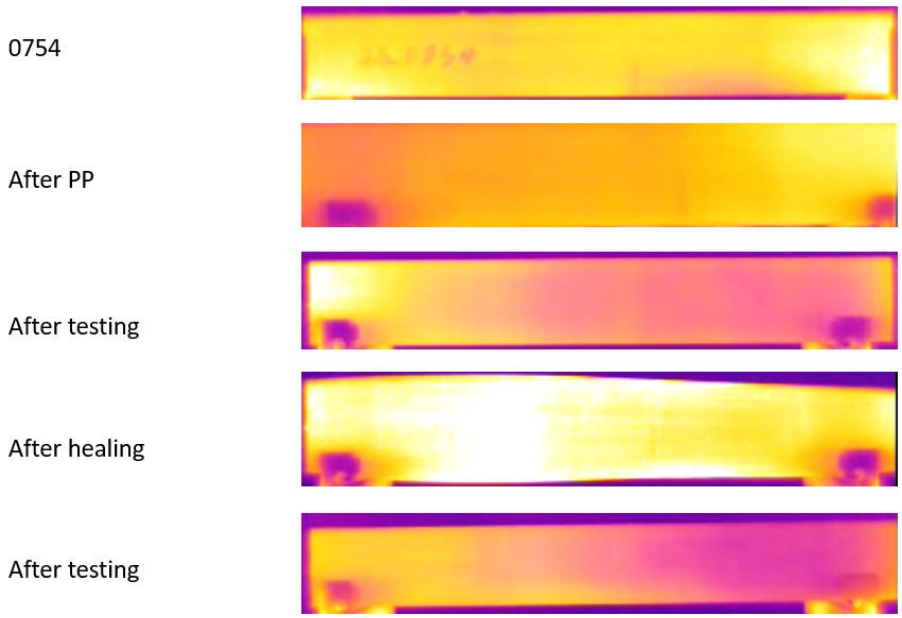

Figure 5.8 Specimen 0754 thermal photos

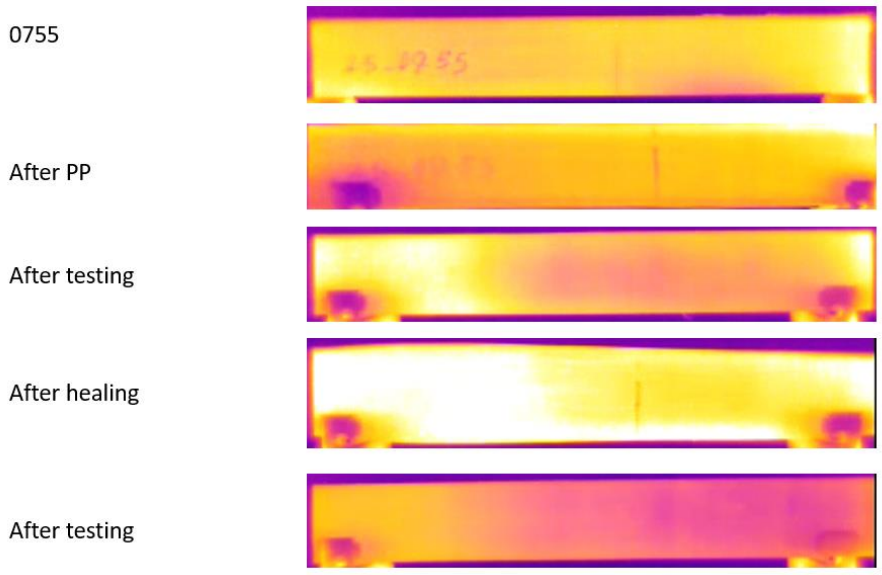

Figure 5.9 Specimen 0755 thermal photos

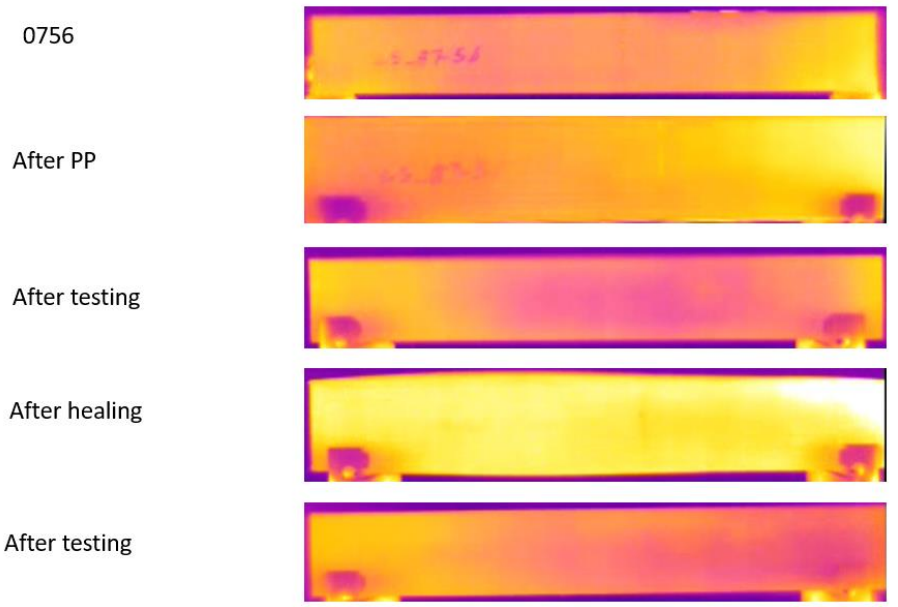

Figure 5.10 Specimen 0756 thermal photos

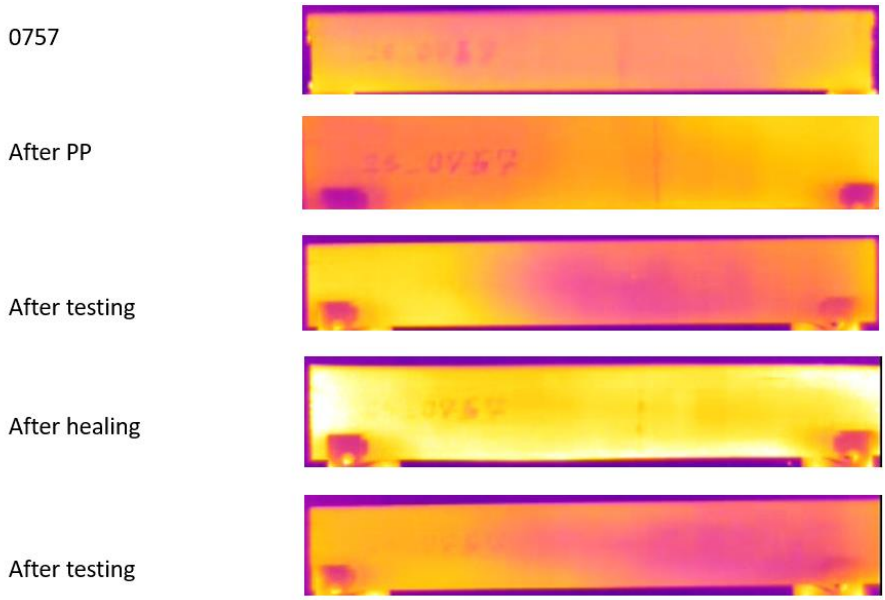

Figure 5.11 Specimen 0757 thermal photos

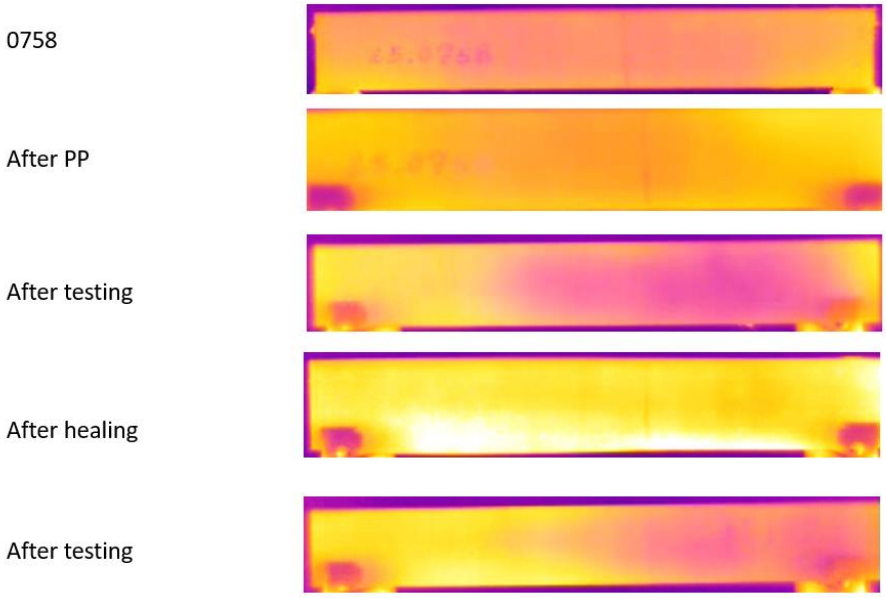

Figure 5.12 Specimen 0758 thermal photos

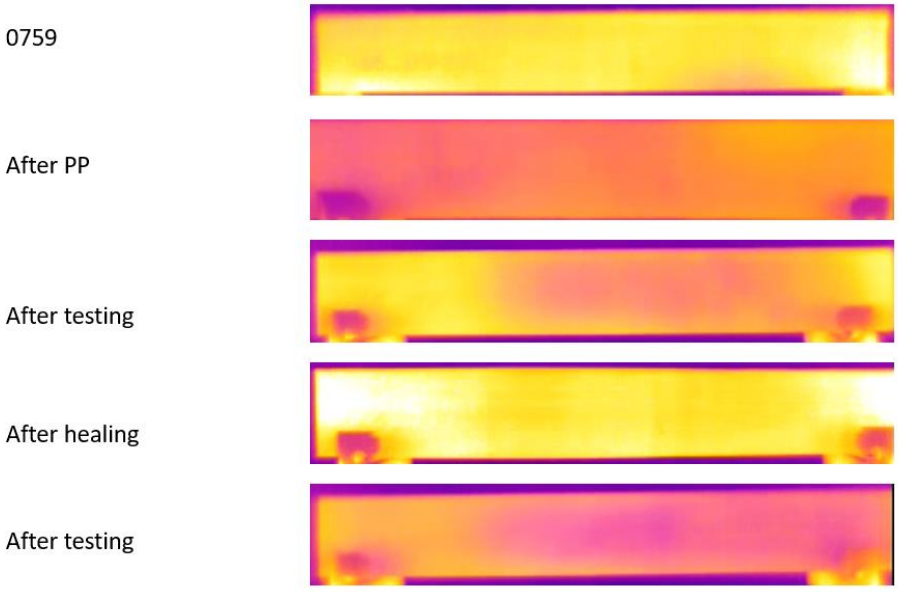

Figure 5.13 Specimen 0759 thermal photos

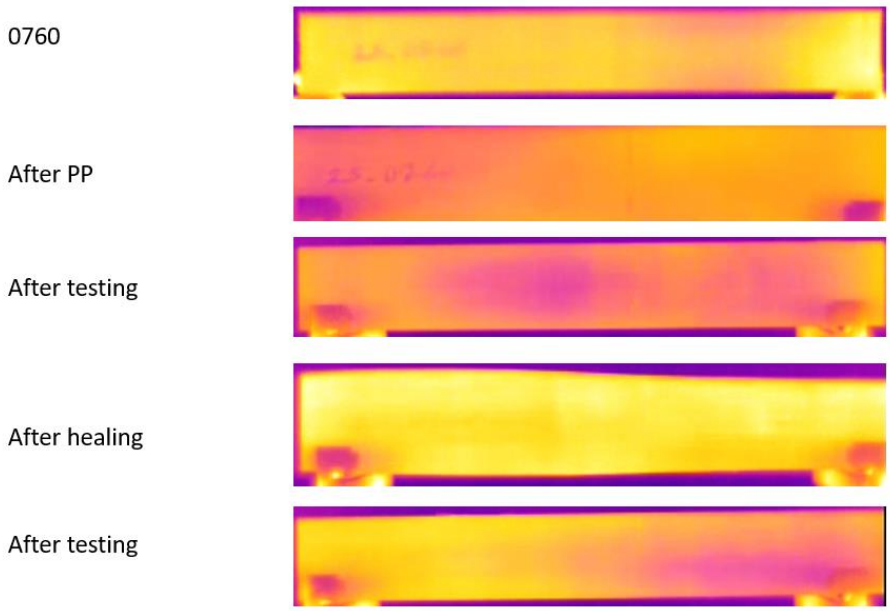

Figure 5.14 Specimen 0760 thermal photos